Arch. Metall. Mater. **63** (2018), 3, 1141-1152

DOI: 10.24425/123787

A.R. SUBHANI*, D.K. MONDAL**#

EFFECT OF REPEATED AUSTENITISATION AND COOLING ON THE MICROSTRUCTURE, HARDNESS AND TENSILE BEHAVIOUR OF 0.16 WT % CARBON STEEL

Repeated austenitisation and furnace cooling of homogenised 0.16 wt. % carbon steels result in ferrite grain sizes between 27 μm and 24 μm. Similarly, repeated austenitisation and normal-air cooling produces ferrite grain sizes between 17 μm and 12 μm; while repeated austenitisation and forced-air cooling produces a minimum grain size of 9.5 μm. Furnace cooling decomposes the austenite eutectoidally to lamellar pearlite; while normal-air cooling and forced-air cooling after austenitisation cause degeneration of pearlite regions producing grain boundary network as well as cluster of cementite and other carbides. Forced-air cooled samples provide the highest YS (364 MPa) and UTS (520 MPa); while furnace cooling provides the lowest (290 MPa and 464 MPa) leaving the normal-air cool performance in between. Hardness values depict the role of individual ferrite and pearlite content and the extent of pearlite degeneration occurring after each cyclic treatment.

Keywords: Ferrite grain size, Pearlite degeneration, Hardness, Tensile behaviour

1. Introduction

The phases available in the microstructure of steels get blended through solidification and subsequent processing which includes hot or cold working, heat treatment and solid-state phase transformation. The composition of steels also matters in changing the phase relationship and microstructure thus providing scopes for various applications. The fortuitous high temperature stability of austenite in steels and its transformation upon cooling at various rates are the basis of optimizing the shape and size of the transformation products and finally to develop microstructures and properties for various applications [1]. If slow cooled under conditions approaching equilibrium, austenite will change to a mixture of polygonal ferrite and coarse pearlite. However, accelerated cooling decreases the austenite to ferrite transformation temperature and promotes ferrite nucleation rate within and around the austenite grains, thereby producing lath or acicular ferrite along with grain refinement [2-6]. The increased cooling rate also favours the non-equilibrium precipitation of finer carbides from the supersaturated austenite and they cannot grow much because of reduced carbon diffusion [3,6] at lower transformation temperatures. The use of micro-alloying elements (niobium, vanadium, and/or titanium) and hot rolling may also lead to production of finer ferrite grains through precipitation of carbides and carbo-nitrides [4,6,7]. As pointed out by Mishra et al [8,9] during their study on niobium micro-alloyed steels, intermediate and high cooling rates can produce lath type bainitic ferrite and degenerated pearlite together with conventional lamellar pearlite. Formation of degenerated pearlite usually relates with the nucleation of cementite at ferrite-cementite interfaces within a transformation temperature range between normal pearlite and upper bainite [10]. The cementite thickness in degenerated pearlite happens to be thinner as compared to the continuous pearlite, and hence gives rise to high strength as well as improved toughness [9]. Although the cementite is characterised by its hard and brittle nature, it can endure large strain when appearing as thin platelets [11]. Beside this, the finer precipitates formed in the ferrite matrix during faster cooling cause work hardening through strain gradient developed near the precipitates due to formation of dislocation loops [12,13] and so play additional role to better the yield strength and toughness. Improvement in strength and work hardening rate also relate with the progress of ferrite grain refinement [12]; while the higher ferrite contiguity ratio is expected to impart better toughness [14-16]. In summary, the resulting strength and toughness of low and medium carbon steels after different treatments used to bear the influence of cooling rate on the transformation of austenite to various micro-constituents.

Considering the prevailing property requirements of a 0.16 wt % carbon steel, the authors have attempted to produce a series of ferrite grain size using the technique of repeated austenitisation followed by cooling at varying rates. The objective is to derive the influence of the said treatments towards development of ferrite grain size and pearlite degeneration. The

* RESEARCH SCHOLAR, METALLURGICAL AND MATERIALS ENGINEERING DEPARTMENT, NATIONAL INSTITUTE OF TECHNOLOGY, DURGAPUR, INDIA
** METALLURGICAL AND MATERIALS ENGINEERING DEPARTMENT, NATIONAL INSTITUTE OF TECHNOLOGY, DURGAPUR, INDIA
# Corresponding author: dk_mondal2003@yahoo.co.in

present study also suggests link between the microstructure so achieved and the mechanical properties, namely, hardness and tensile strength.

2. Experimental procedure

Hot rolled steel bars of square (13 mm × 13 mm) cross-section and bearing composition given in Table 1 were homogenised at 1423 K for 90 min and subsequently furnace cooled at a controlled rate of 278 K per min. The homogenised bars were sectioned to smaller specimens of 10 mm length and subjected to repeated austenitisation and cooling cycles for 1, 3, 5 and 7 times where the rate of cooling was varied from furnace cooling to normal air cooling and then to forced air cooling. Table 2 enlists the designated treatments detailing the cycles of austenitisation and cooling performed during each treatment.

TABLE 1

Chemical composition, wt%

C	Mn	Si	Ni	Cr	Mo	V	S	P	Cu	Nb	Fe
0.16	1.32	0.24	0.04	0.06	0.006	0.052	0.006	0.026	0.001	0.015	98.0

TABLE 2

Designated heat treatments to develop microstructures with varying grain size and pearlite morphology

Designated Treatments	Steps or Treatment Cycles
Homogenised	Austenitise the hot rolled steel at 1423 K for 90 min, furnace-cool at a controlled rate (5°C/min) up to 773 K, and then cool to room temperature.
FC-1cy	Austenitise the homogenised steel at 1223 K for 10 min, furnace cool up to 773 K.
FC-3cy FC-5cy FC-7cy	Repeat the above cycle of austenitisation and furnace cooling for 3, 5 and 7 times, respectively, and then cool to room temperature.
AC-1cy	Austenitise the homogenised steel at 1223 K for 10 min, cool in normal air up to room temperature.
AC-3cy AC-5cy AC-7cy	Repeat the above cycle of austenitisation and air-cooling for 3, 5 and 7 times, respectively.
FAC-1cy	Austenitised the homogenised steel at 1223 K f or 10 min, force-air cool to room temperature using air flow rate of 4.17×10^{-3} m^3 per second.
FAC-3cy FAC-5cy FAC-7cy	Repeat the above cycle of austenitisation and force-air cooling for 3, 5 and 7 times, respectively.

For microstructural investigation, samples were prepared using standard metallographic techniques, etched with 2% Nital and later examined under light as well as scanning electron microscopes equipped with EDS facility for analysis on selected areas or phases. Volume percent of ferrite and pearlite were determined by counting of the phases at 450X magnification with the help of an automatic point counter fitted with an light microscope. While the ferrite grain size was determined in terms of average grain diameter following standard ASTM practice (see appendix 1) and by counting nearly 500 grains at 450X for each sample. Tensile tests were carried out in duplicate in an Instron machine of 100 kN capacity using standard flat specimens at a crosshead speed of 1mm per min and full-scale load of 100 kN. The ultimate tensile strength (UTS), yield strength (YS) and total elongation (TE) values were determined from the corresponding load-elongation plots by taking an average of two measurements. Bulk hardness was measured under 294 N load in a Vickers hardness tester and averaged from at least five readings on each sample.

3. Results and discussion

3.1. Light Microscopy

Fig. 1a shows light micrograph of the experimental steel subjected to homogenisation treatment revealing polygonal ferrite and coarse lamellar pearlite as primary micro-constituents. In contrast, repeated austenitisation and furnace cool treatments (FC-1cy, FC-3cy, FC-5cy and FC-7cy) have produced relatively smaller ferrite grains and pearlite areas (Fig. 1b-e). There is a gradual decrease in both ferrite grain diameter and pearlite size with increase in cycle numbers from 1 to 7. The said treatments also provide thin white film of carbide along the ferrite grain boundaries, thus joining two pearlite regions as illustrated in Fig. 1f.

On increasing the cooling rate after austenitisation, i.e., during AC-1cy, AC-3cy, AC-5cy and AC-7cy treatments, there has been a tendency towards overall refinement of the microstructure explicitly as function of the number of repeating cycles. This produces smaller ferrite grains along with pearlite regions appearing as dispersed particles as well as thin grain boundary envelops (Fig. 2a-d). It is likely that the repeating austenitisation of an air-cooled structure at a lower temperature of 1223 K for 10 min during 3-, 5- and 7-cycle treatment causes insignificant growth of the austenite grains, which on subsequent air-cooling transforms to an aggregate of finer ferrite and dispersed pearlite. With further increase in the cooling rate during FAC-1cy, FAC-3cy, FAC-5cy and FAC-7cy treatments, the resulting ferrite grains become much smaller and distorted to form acicular / lath shape leaving the pearlite areas sandwiched between these laths (Fig. 3a-d). The degree of distortion to form acicular ferrite appears to be quite prominent with increasing the number of repeating cycles. Repeated austenitisation of the force-air cooled structure during 3, 5, and 7 cycle treatment is expected to produce well refined austenite grains which on final forced air cooling from 1223 K transforms to still finer ferrite with distortion and pearlite with greater dispersion. In addition, repeated austenitisation – forced air cool treatment results in typical degeneration of pearlite regions as illustrated in Fig. 3e for FAC-7cy treatment. It is likely that the enhanced cooling rate during normal and forced-air cooling after austenitisation provides greater under-cooling as a driving force

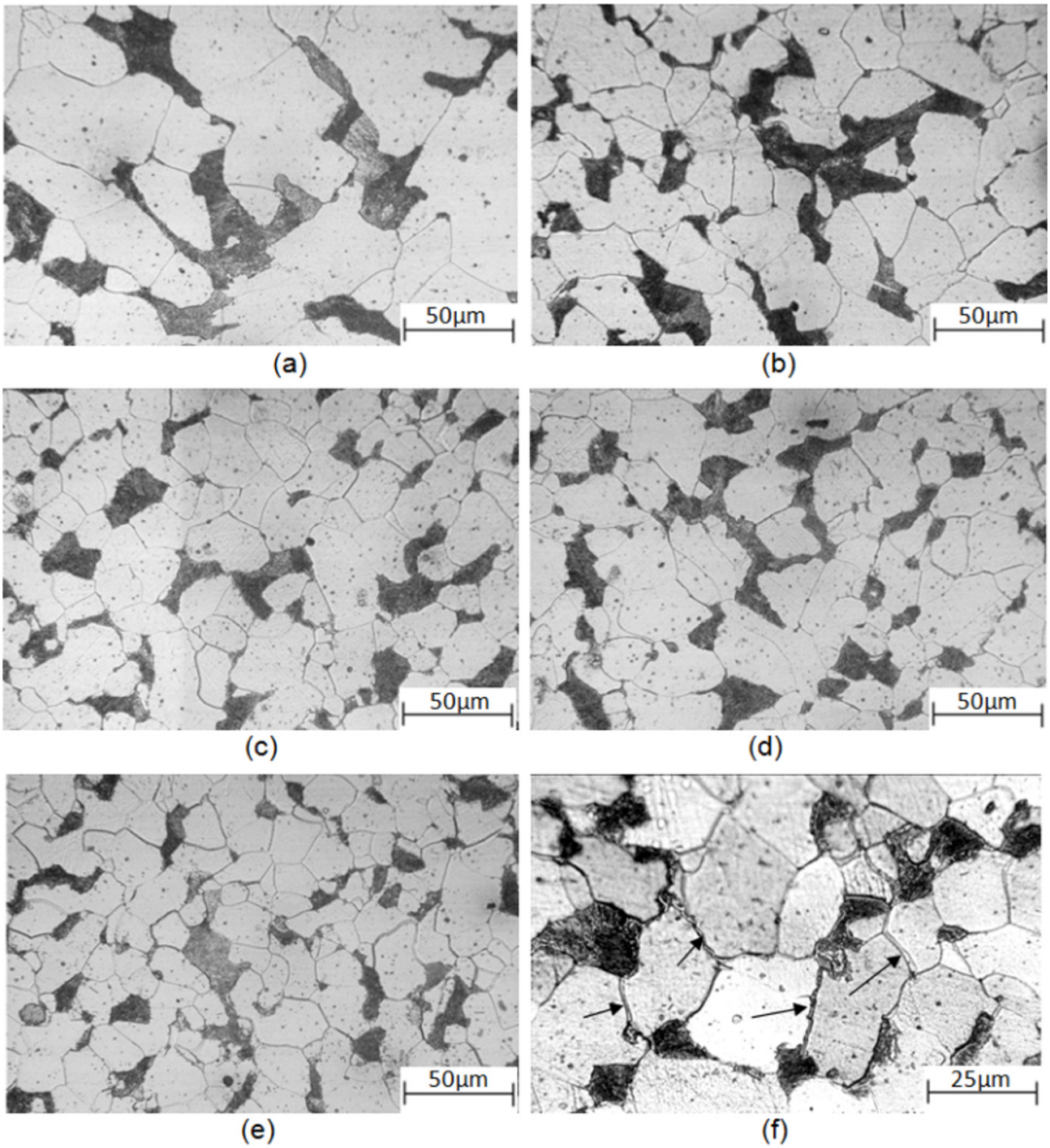

Fig. 1. Representative light micrographs of steels subjected to (a) Homogenisation Treatment, (b, f) FC-1cy treatment, (c) FC-3cy treatment, (d) FC-5cy treatment, and (e) FC-7cy treatment

for non-equilibrium transformation [8,9,17] of the austenite to degenerated pearlite producing clusters of carbides. The forced-air cooled microstructure in Fig. 3e also shows precipitated carbides dispersed all through the ferrite matrix. Researchers [8,9] have already identified these carbides as vanadium carbide in vanadium micro-alloyed steels and niobium carbides in niobium micro-alloyed steels. Since the experimental steel is micro-alloyed with vanadium as well as niobium, the precipitates appearing in Fig. 3e following FAC-7cy treatment are likely to contain either of these two elements or both.

3.2. Scanning Electron Microscopy

To proceed for microstructural analysis, the homogenised microstructure (Fig. 4a), being an initial microstructure revealing coarse lamellar pearlite with polygonal ferrite, has been chosen as a reference microstructure; so that the features developed after different cyclic treatments can be characterised through comparison with this reference microstructure. Based on this concept, a close look at Fig. 4a and b suggests that the FC-1cy treatment does not cause any significant change to the

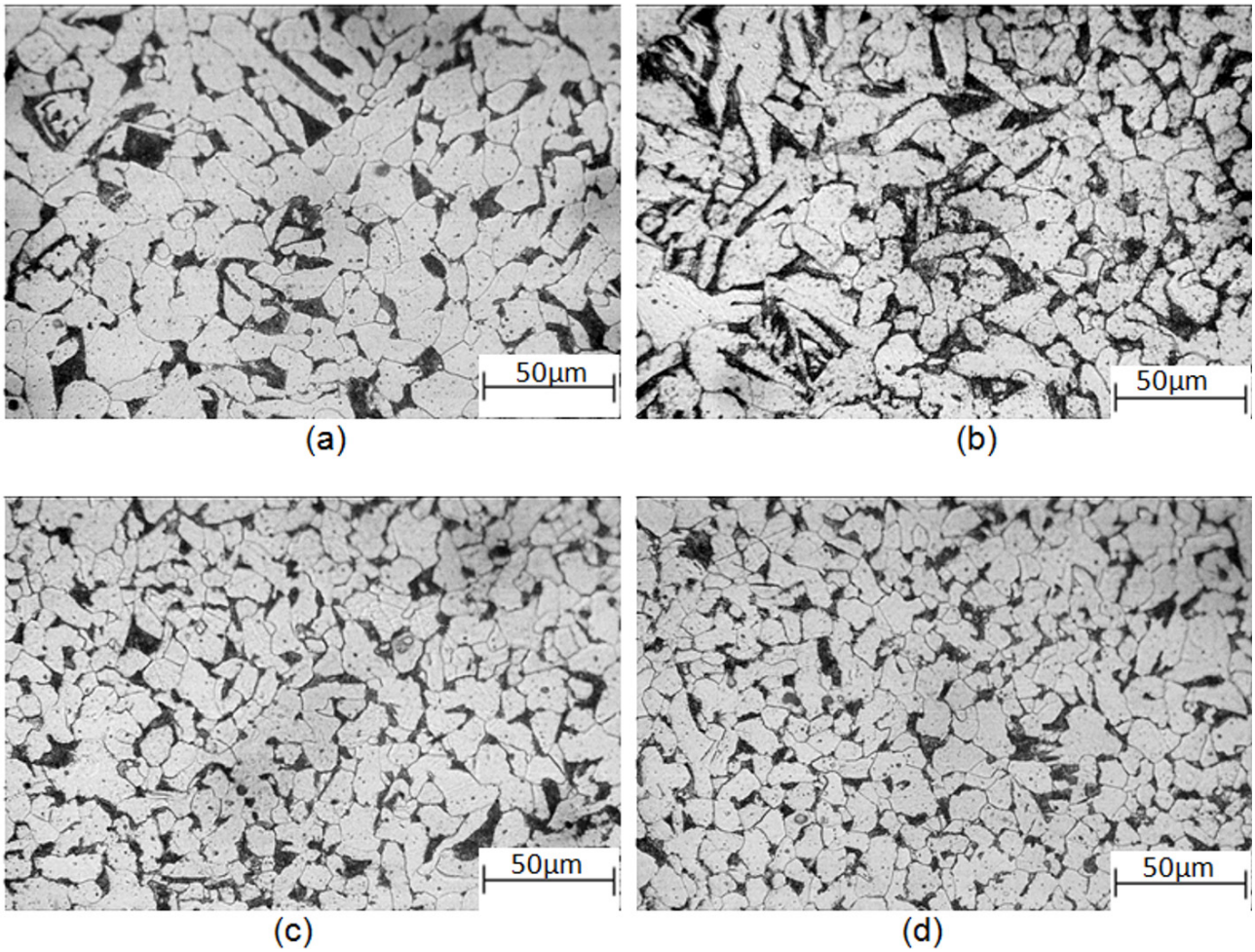

Fig. 2. Representative light micrographs of steels subjected to (a) AC-1cy treatment, (b) AC-3cy treatment, (c) AC-5cy treatment, and (d) AC-7cy treatment

initially homogenised microstructure with reference to ferrite grain size and pearlite pattern. However, with increase in the number repeating cycles from 1 to 5, the lamellar pattern of the ferrite-carbide in pearlite colonies modifies partly to produce grain boundary carbide network as illustrated in Fig. 4c,d. Subsequently, the FC-7cy treatment causes nominal change to the ferrite grain size but degeneration of only thinner pearlite producing fresh ferrite fields encapsulated by white network of cementite (Fig. 4e). It is necessary to mention that austenitisation and furnace cooling for 3, 5 and 7 cycles reduce the saturation limit for solubility of carbon and alloying elements in the austenite. This leads to a situation facilitating precipitation of carbides with increased repeating cycles (Fig. 4c-e). EDS analysis carried out only on a FC-5cy treated sample suggests the possibility of forming grain boundary carbide (*point 1* in Fig. 5a) containing 0.12 wt.% niobium with traces of other elements (S, P ,Si and Mn) arising out of the composition of the initial austenite. Whereas, the clustered carbide at the ferrite – pearlite interface (*point 4* in Fig. 5a) appears to be of iron-carbide containing traces of vanadium, niobium and other elements. Similarly, the ferrite matrix (*point 2* in Fig. 5a) maintains a composition with minimum concentration of any element; while the precipitate on it bearing greater concentration of iron, manganese and sulphur (*point 3* in Fig. 5a) shows the possibility of forming $(Fe, Mn)_3 S$.

SEM micrographs given in Fig. 6a-d clearly reveal finer ferrite grains along with grain boundary network and cluster of carbides as a mark of pearlite degeneration occurring during repeated austenitisation and air cooling treatment. The pearlite degeneration appears to be much more progressive in thinner regions as compared to massive regions of pearlite. The massive pearlites exhibit partial degeneration modifying the majority of lamellar carbides to smaller segments or near spherical shape particularly after 3 and 5 – cycle treatments. It is important to note that before conduct of cycle-3 in AC-3cy treatment the steel is subjected to cycle-2 treatment involving austenitisation and normal-air cooling to produce grain-refined ferrite and partially degenerated pearlite regions. The short segments of thin lamellar carbides in a partially degenerated pearlite usually contain increased number of faults or defect enriched regions. Such defect-enriched segmented carbides readily break in to still smaller segments or near spherical shape following diffusion of carbon from faulted regions to the adjacent austenite during austenitisation in subsequent cycles [18]. Occurrence of the above features is very much evident in Fig. 6b and c following pearlite degeneration after AC-3cy and AC-5cy treatments.

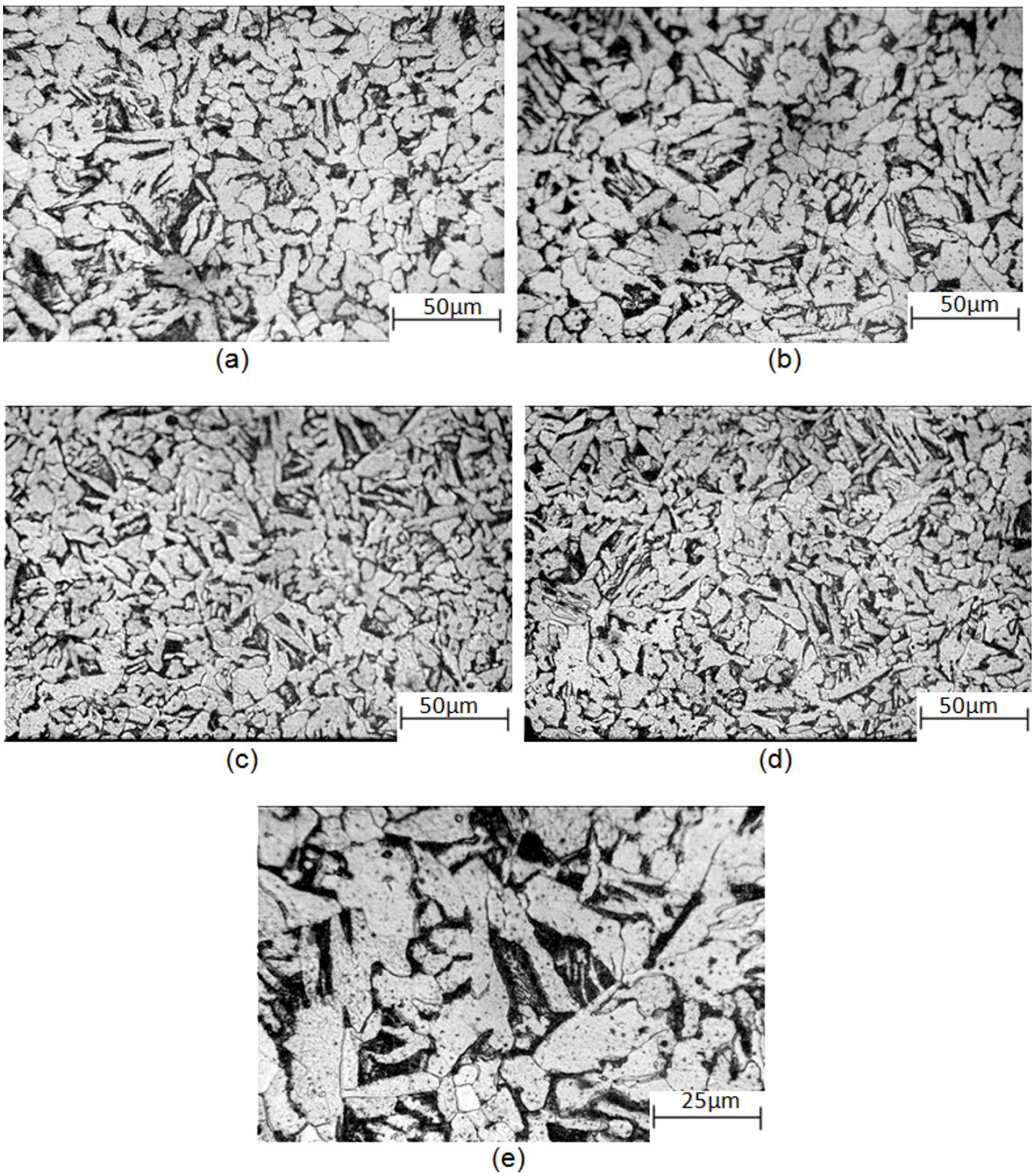

Fig. 3. Representative light micrographs of steels subjected to (a) FAC-1cy treatment, (b) FAC-3cy treatment, (c) FAC-5cy treatment, (d) FAC-7cy treatment, and (e) FAC-7cy treatment (at high magnification)

Intense pearlite degeneration after AC-7cy treatment produces regions almost devoid of carbide plates or lamellae and there occurs spherical carbides along with interface precipitation of carbide between the degenerated pearlite and the matrix ferrite. Interface precipitation of carbide occurs quite profusely after repeated austenitisation – forced-air cool (FAC) treatment as evident in Fig. 7a-d. Apart from interface precipitation, grain-boundary cementite network and carbide clustering as a mark of pearlite degenerated appear as additional features in the said figures. Incidentally, the said carbides remain un-dissolved on subsequent short duration (10 min) austenitisation at 1223 K during multi-cycle treatment. The austenite with un-dissolved cementite or other carbides experiences divorced eutectoid transformation [19,20] following forced air cooling to produce cluster of cementite plates embedded on a ferrite matrix instead of lamellar ferrite-carbide aggregate. Pearlite degeneration also causes localised bulging along the carbide network possibly through diffusion of carbon and other elements within the net-

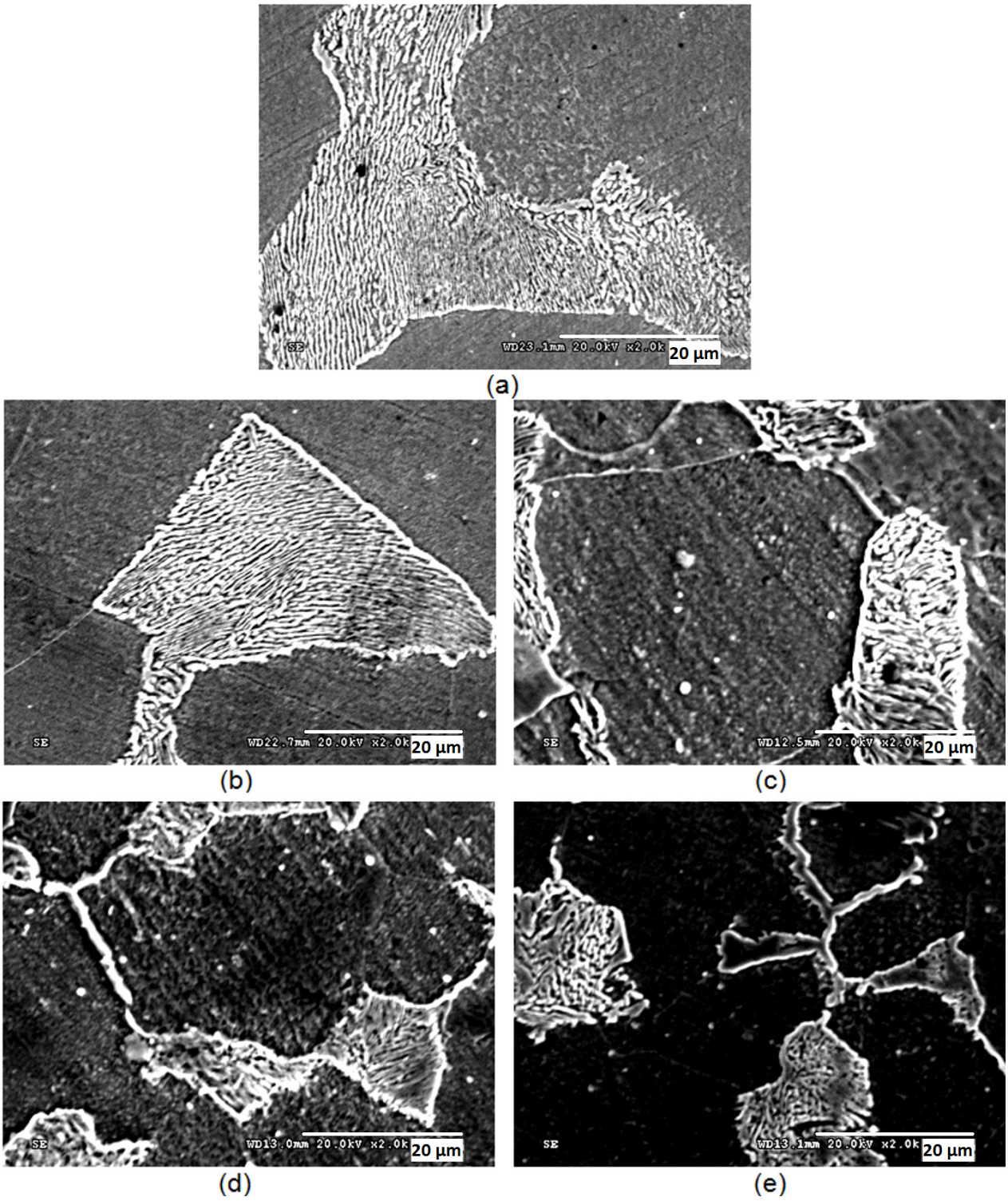

Fig. 4. SEM secondary electron images of the steels subjected to (a) Homogenisation Treatment, (b) FC-1cy treatment, (c) FC-3cy treatment, (d) FC-5cy treatment, and (e) FC-7cy treatment

work itself. As a result, carbide segments with inflated/spherical regions appear randomly as indicated in Fig. 7d. Dissolution of these carbides is quite sluggish during austenitisation in cyclic treatment [21], instead they experience growth by the coagulation process following the Ostwald ripening phenomenon [22]. Following EDS analysis carried out on FAC-5cy treated sample, an isolated carbide (*point 1* in Fig. 5b) appears to contain mainly iron and manganese along with sulphur thus resembling the composition of $(Fe, Mn)_3$ S. Whereas, the carbide appearing as network (*point 2* in Fig. 5b) exhibits mainly iron along with manganese and vanadium as trace elements. Residual carbide in a degenerated pearlite (*point 3* in Fig. 5b), though containing iron and nominal manganese, happens to be devoid of sulphur, vanadium and niobium possibly because of their diffusion towards grain boundary regions during austenitisation treatment.

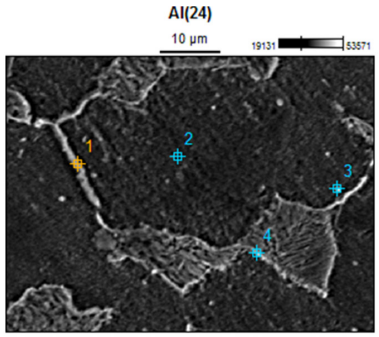

(a)

	C-K	Al-K	Si-K	P-K	S-K	V-K	Mn-K	Fe-K	Ni-K	Cu-K	Nb-L
pt1	0.03	0.00	0.13	0.09	0.06	0.00	0.35	68.58	0.00	0.00	0.12
pt2	0.00	0.02	0.06	0.06	0.00	0.00	0.61	68.63	0.06	0.00	0.07
pt3	0.00	0.00	0.13	0.05	9.35	0.02	18.65	35.51	0.00	0.14	0.00
pt4	0.08	0.05	0.13	0.04	0.00	0.04	0.49	68.53	0.15	0.12	0.03

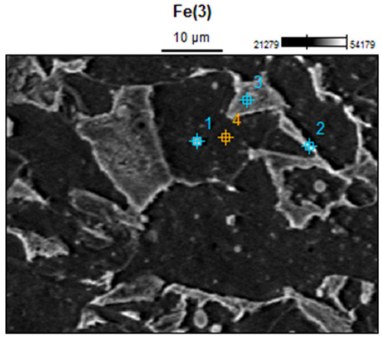

(b)

	C-K	Al-K	Si-K	P-K	S-K	V-K	Mn-K	Fe-K	Ni-K	Cu-K	Nb-L
pt1	0.00	0.04	0.04	0.00	13.76	0.00	26.77	20.21	0.00	0.34	0.00
pt2	0.00	0.00	0.10	0.05	0.02	0.03	0.48	68.56	0.00	0.00	0.00
pt3	0.00	0.01	0.10	0.09	0.00	0.00	0.53	69.05	0.00	0.00	0.00
pt4	0.00	0.06	0.09	0.07	0.00	0.00	0.43	69.15	0.00	0.00	0.07

Fig. 5. EDS analysis of the precipitates or carbides occurring at different locations in (a) FC-5cy sample and (b) FAC-5cy sample

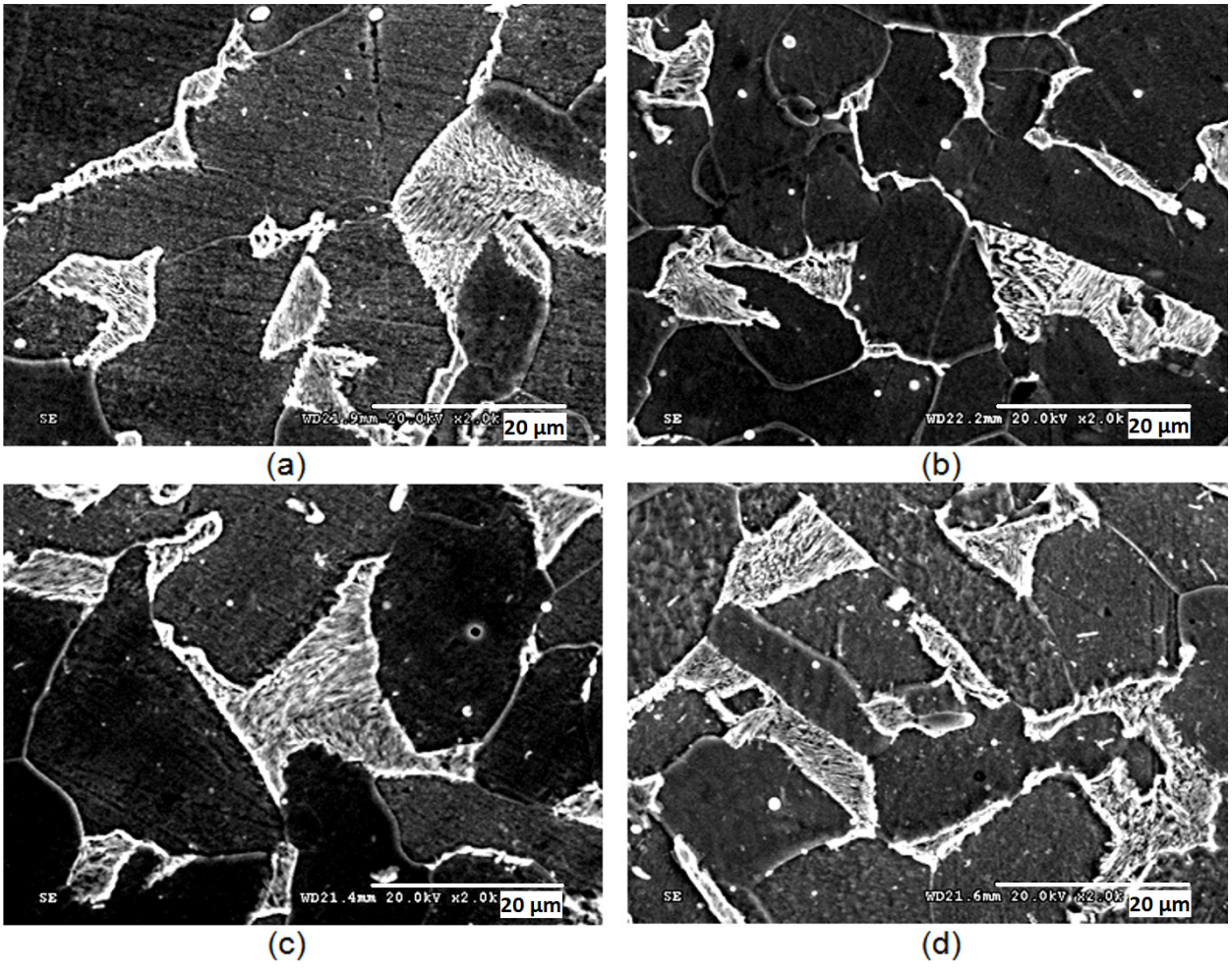

Fig. 6. SEM secondary electron images of the steels subjected to (a) AC-1cy treatment, (b) AC-3cy treatment, (c) AC-5cy treatment, and (d) AC-7cy treatment

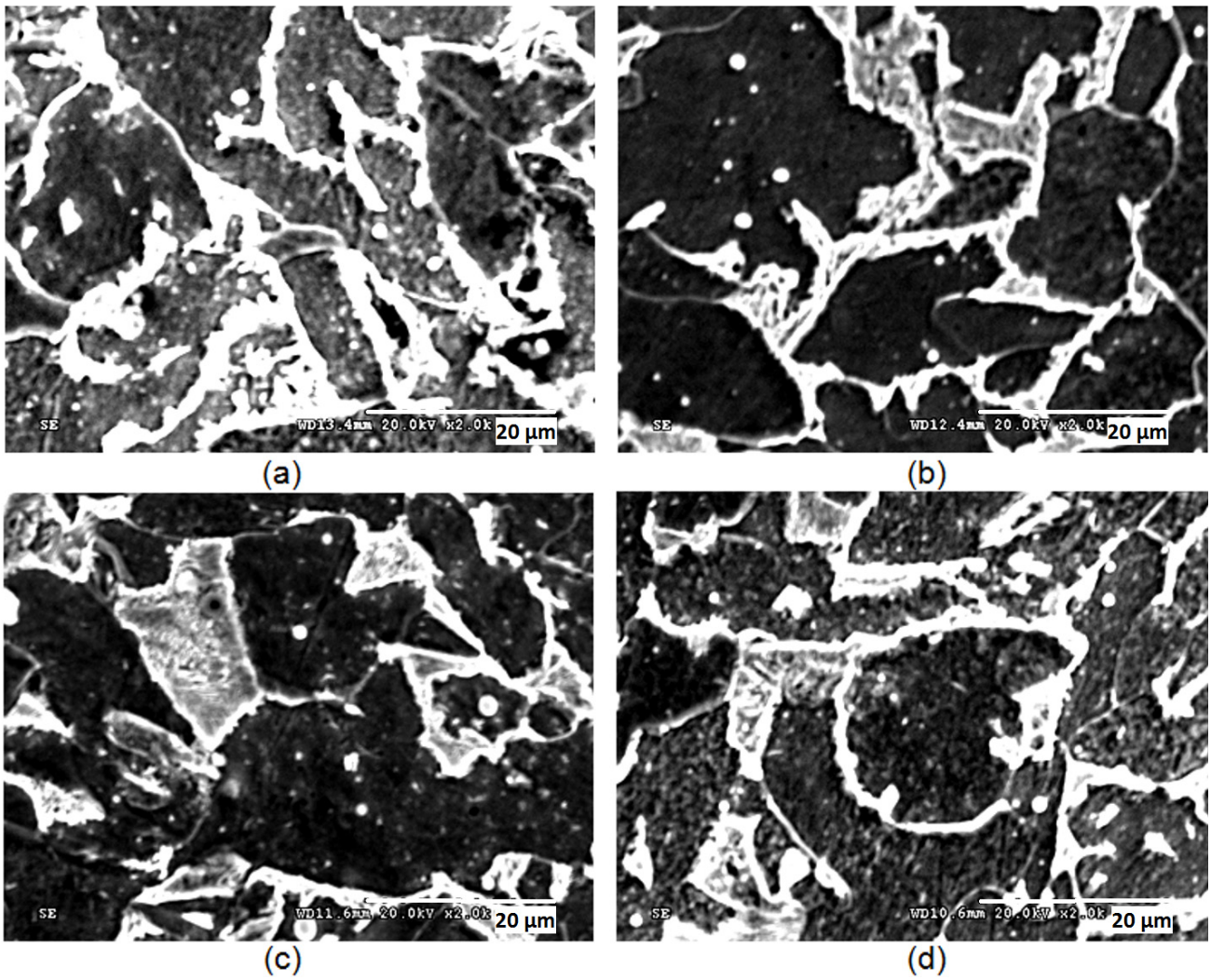

Fig. 7. SEM secondary electron images of the steels subjected to (a) FAC-1cy treatment, (b) FAC-3cy treatment, (c) FAC-5cy treatment, and (d) FAC-7cy treatment

3.3. Ferrite grain size

As depicted in Table 3, homogenisation treatment at 1423 K produces the largest ferrite grain diameter of 45 µm. FC-1cy treatment of the homogenised steel reduces the average grain diameter drastically to 27 µm. However, repeating austenitisation and furnace cooling up to 7 times causes an insignificant drop in grain size to 24 µm. In contrast, repeating austenitisation – normal-air cooling treatment for 1, 3, 5 and 7 cycles reduces the average grain diameter moderately to one ranging between 17 µm and 12 µm. Use of forced- air cooling (FAC) instead of normal air cooling after austenitisation causes further reduction in average grain diameter, thus producing a minimum average grain diameter of 9.5 µm after FAC-7cy treatment. In all the cyclic treatments, when the initially homogenised steel is austenitised at 1223 K, the ferrite-pearlite interfaces act as potential sites for austenitisation [23]. Simultaneously, austenitisation takes place at the ferrite-cementite interfaces in pearlite regions. In both cases, the ferrite phase rapidly changes to austenite in a diffusion-less polymorphic transformation [24] at 1223 K. On continued holding at this temperature, dissolution of cementite in the austenite phase is a diffusion controlled slow process. In the present study, austenitisation at 1223 K for an inadequate period of 10 min causes incomplete dissolution of the pearlitic cementite or the isolated carbides appearing in the initially homogenised microstructure. The presence of any un-dissolved cementite or other carbide ceases the austenite growth during holding at 1223 K. On subsequent furnace cooling, the inadequately grown austenite experiences less under-cooling, thereby transforming to ferrite with nominal reduction in grain size. However, on subsequent air-cooling, the austenite gets under-cooled largely below the critical transformation temperature and transforms to numerous ferrite nuclei, whose growth ceases rapidly to produce finer grains. The more intense under-cooling due to forced-air cooling after austenitisation causes typical modification of the ferrite grains from polygonal to acicular shape in addition to their refinement.

Further, it is apparent from graphical representation in Fig. 8 that though the initial (homogenised) grain diameter has dropped largely by 1cycle treatment at all cooling rates, fall in grain diameter in subsequent cycles happens to be quite gradual. In all cases of cyclic treatment, holding at 1223 K for 10 min produces

TABLE 3

Average grain diameter of ferrite versus % ferrite and % pearlite after various treatments**

Designated Treatment	Av. grain dia, μm	% Ferrite	% Pearlite (lamellar + degenerated)
Homogenised	45	82	18
FC-1cy	27.0	80	20
FC-3cy	25.8	82	18
FC-5cy	25.2	82	18
FC-7cy	24.0	85	15
AC-1Cy	17.13	73	27
AC-3Cy	14.9	76	24
AC-5Cy	14.7	79	21
AC-7Cy	12.5	83	17
FAC-1Cy	15.23	70	30
FAC-3Cy	13.95	70	30
FAC-5Cy	13.26	76	24
FAC-7Cy	9.5	76	24

** Reported values are in the range of ±2.0

austenite grains with inadequate growth for reasons described earlier. In addition, there is a limit to the extent of austenite grain refinement following repeated austenitisation after each cooling cycle even at a rate corresponding to forced-air cooling. Fig. 8 clearly depicts that the austenite grain size ceases to drop after 3-cycles of each designated treatment, thereby resulting in no major change in ferrite grain size on transformation beyond 3 cycles of treatment. Beside this, forced-air cooling marginally supersedes the normal-air cooling performance towards refining the ferrite grain size, thus generating quite close values of minimum grain diameters, i.e. 12.5 μm and 9.5 μm after AC-7cy and FAC-7cy treatment, respectively.

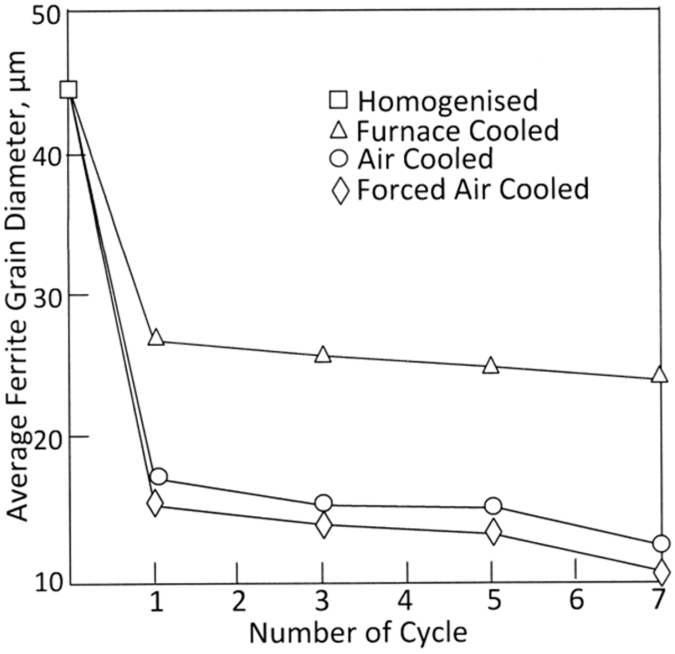

Fig. 8. Variation of ferrite grain size with cooling rate and number of cycle

3.4. Quantitative metallography

Following quantitative estimation of ferrite and pearlite in Table 3, it appears that not much change to the content of these two micro-constituents has taken place after repeated austenitisation – furnace cool treatment of the homogenised steel. In contrast, AC-1cy treatment results in a moderate rise in pearlite content from an initial value of 18% (for homogenised steel) to 27%, which later reduces to 24, 21 and 17% with increasing repeating cycle from 1 to 3, 5 and 7, respectively. In fact, air-cooling after austenitisation provides a situation favouring non-equilibrium transformation of the austenite phase, thereby raising the pearlite content to 27% after AC-1cy treatment. At the same time, there is degeneration of pearlite regions with increased severity following the rise in cycle number from 1 to 7. This produces separate masses of ferrite and carbide in a degenerated pearlite. As a result, AC-7cy treatment gives rise to a fall in pearlite content from 27% to 17% and a corresponding gain in ferrite phase. The said non-equilibrium situation also arises quite actively during austenitisation – forced-air cool cycle thus enhancing the pearlite content up to 30% after bothFAC-1cy and FAC-3cy treatment. Such an increase in pearlite content in the forced-air cooled samples accounts for dispersion of pearlite areas and counting of pearlite regions during point counting irrespective of the phenomenon of degeneration. In fact, identifying degenerated pearlite with clear details during counting of phases at low magnification (450 X) becomes difficult for FAC-1cy and FAC-3cy treated samples and so counting in that respect does not arise. However, severe degeneration of the pearlite during FAC-5cy and FAC-7cy treatment causes clear segregation of the ferrite and carbide phases and this makes more counting on ferrite phase possible during point counting process and subsequent fall in pearlite content to 24% quite feasible.

3.5. Tensile behaviour

As reported in Table 4, homogenisation treatment gives rise to a minimum YS of 256 MPa and UTS of 450 MPa with 30% elongation attributing these values to the greatest ferrite grain size of 45 μm. However, after FC-1cy, AC-1cy and FAC-1cy treatments the average grain diameter falls to 27 μm , 17 μm and 15 μm thereby escalating the corresponding YS(UTS) combination to 290(464) MPa, 318(472) MPa and 342(500) MPa, respectively, with practically no loss in the elongation. After repeating the said treatments for 3 and 5 times, the average grain diameter reduces further to enhance the YS (UTS) combination at the peak value of 310(496) MPa after FC-5cy treatment followed by the next higher values of 340(510) MPa and 364(520) MPa after AC-5cy and FAC-5cy treatment, respectively. It is, therefore, likely that the reduced grain sizes developed by 5 times repetition of the designated treatments definitely play a key role towards achieving improved YS and UTS without incurring any loss in ductility or elongation values. Further, it would not be wise to rule out the role of microstructural features produced by

pearlite degeneration in normal-air cooled and forced-air cooled samples towards monitoring the property data. For example, the marginal fall in YS and UTS after AC-7cy and FAC-7cy treatments attributes mainly to the increased ferrite content (Table 3) following severe pearlite degeneration and partly to the grain boundary sliding to relieve strain-hardening effect while testing steels containing greater grain boundary areas [25]. Thus, the extent strengthening of the experimental steel without incurring any loss to its inherent ductility correlates partly with the ferrite grain size and partly to the extent of pearlite degeneration occurring after various cyclic treatments. In addition, the hardness and abrasion resistance of the network and clustered carbides obtained by pearlte degeneration in normal and forced-air cooled samples have a definite bearing for improved mechanical properties; while the ductile as well as tough acicular ferrite particularly in forced-air cooled sample arrest crack growth and toughens the total material. Besides, in air-cooled samples the non-equilibrium precipitation of finer carbides from the austenite also plays a positive role to increase YS values.

Fig. 9a shows tensile fracture representing ductile tearing for the homogenised steel, which forms shallow and large cavities by void coalescence. Fracture surfaces (Fig. 9b,c) after repeated austenitisation and furnace cool treatment also contain ductile tearing but with smaller cavities along with some regions resembling cleavage pattern possibly due to grain boundary concentration of carbides following pearlite degeneration. In contrast, fracture surfaces after repeated austenitisation – air cool treatment assume typical inter-crystalline pattern involving a large number of small size dimples or voids as illustrated in Fig. 9d,e. To describe the effect of cooling rate on the fracture behaviour of micro-alloyed steels, Sanmugam et al. [9] correlated this pattern of fracture with greater micro-plasticity associated with bainitic pattern of the ferrite phase. Evidently, the same mechanism of tensile fracture through micro-dimple formation appears in case of forced-air cooled samples where the density of micro-voids increases with increase in the number of repeating cycle from 1 to 7 (Fig. 9f,g). Fracture surfaces of the forced-air cooled samples also show void sheets produced by micro-void coalescence and regions resembling cleavage facet at the sites of carbide clustering in degenerated pearlite.

3.6. Hardness

Hardness HV151 of the initially homogenised steel corresponds to its near equilibrium proportion of ferrite and lamellar pearlite (82:18) and remains almost unaltered after FC-1cy and FC-3cy treatment in spite of drastic fall in grain size from 45 μm to 25.8 μm. Whereas, after AC-1cy and AC-3cy treatment the initial hardness rises marginally to HV 157 and HV160 following a significant drop in grain size to 17 μm and 15 μm, respectively. Such rise in hardness with decreasing grain size for the air-cooled steels attributes partly to the overall refinement of microstructure and to the rise in pearlite amount (Table 3). However, the reduced pearlite content or, alternately, the rise in ferrite content after 5 and 7 cycle treatment following severe degeneration of pearlite regions gives rise to a hardness fall to a minimum of HV136 in case FC-7cy treatment and HV149 in case of AC-7cy treatment. This particular trend in hardness variation remains missing in case of forced-air cooled samples where the peak hardness (HV156) appears only after FAC-5cy treatment. Although the pearlite content has increased to 30% after FAC-1cy and FAC-3cy treatments (Table 3), it is likely that a major part it experiences degeneration to segregate ferrite and carbide phases and so gives rise to somewhat reduced hardness of HV153. Therefore, considering the role of pearlite degeneration following divorced eutectoid transformation of the austenite, it would be wise to assess the extent of ferrite segregation and carbide clustering along with grain refinement and straining of the ferrite phase while determining the hardness of a forced air-cooled sample. Thus, the FAC-7cy treatment causing extreme grain refinement and straining of the ferrite phase also provides an additional ferrite to the tune of nearly $0.21 \approx (04 \times 0.88)$ after complete degeneration of 24% pearlite (Table 3). Possibly this gives rise to lowering of hardness from the initial higher value of HV156 to HV144 after FAC-7cy treatment.

TABLE 4

Grain size versus tensile test results and hardness values**

Treatment	Grain size, μm	YS, MPa	UTS, MPa	Elongation, %	Hardness, HV
Homogenised	45.0	256	450	30	151
FC-1cy	27.0	290	464	34	152
FC-3cy	25.8	295	464	32	150
FC-5cy	25.2	310	496	33	140
FC-7cy	24.0	306	482	33	136
AC-1cy	17.13	318	472	29	157
AC-3cy	14.9	318	475	33	160
AC-5cy	14,7	340	510	30	154
AC-7cy	12.5	329	490	34	149
FAC-1cy	15.23	342	500	27	153
FAC-3cy	13.95	344	516	32	153
FAC-5cy	13.26	364	520	32	156
FAC-7cy	9.5	356	517	30	144

** Reported Values are in the range of ±5.0%

4. Conclusions

1. Light microstructure containing large polygonal ferrite and coarse lamellar pearlite of homogenised steel continues to occur in steels subjected to repeated austenitisation and furnace cooling. Repeated austenitisation and normal air cooling cause refinement of both ferrite and pearlite regions; while repeated austenitisation and forced-air cooling provides much finer ferrite grains with distortion producing lath ferrite and pearlite sand-witched between the laths.
2. Scanning electron micrographs reveal the formation of carbide network through partial degeneration of pearlite regions after repeated austenitisation and furnace cool

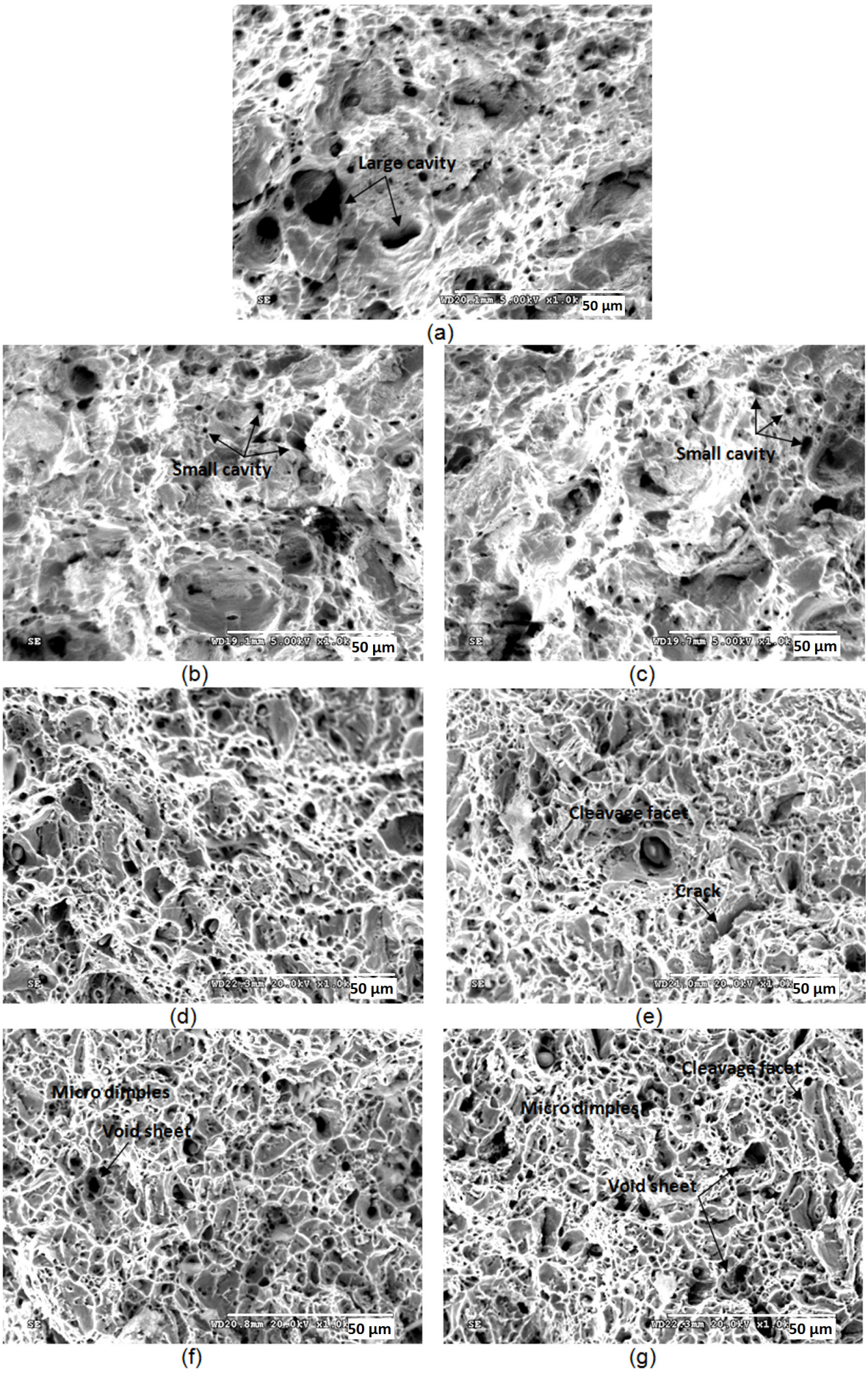

Fig. 9. SEM fractographs of the tensile tested specimens with different treatments

treatment. Extensive degeneration of pearlite after repeated austenitisation and air cooling changes the lamellar carbides within pearlite partly to grain boundary network and partly to cluster form. Complete degeneration of pearlite following repeated austenitisation and forced-air cool practice gives rise to the formation of distinct patches and network of carbide apart from lath ferrite.

3. The largest ferrite grain diameter of 45μm achieved through homogenisation treatment drops moderately to 27 μm by FC-1cy treatment, largely to 17 μm by AC-1cy treatment and further to 15 μm by FAC-1cy treatment. Thereafter, the grain diameter drops nominally with increased repeating cycles of the said designated treatments, thus reaching a minimum of 9.5 μm after FAC-7cy treatment.
4. Near-equilibrium (~80:20) proportion of ferrite and pearlite appearing after homogenisation treatment remains almost unaltered after repeated austenitisation and furnace cooling. Whereas, repeated austenitisation followed by normal-air cooling or forced-air cooling modifies this proportion with irregularities due the prevailing state of non-equilibrium and degeneration of the pearlite regions.
5. A good combination of YS and UTS (340 MPa and 510 MPa) appears after AC-5cy treatment; while FAC-5cy treatment gives rise to the highest YS of 364 MPa and UTS of 520 MPa along with retention of elongation up to 30%. Hardness values, though degraded with increased cycle number of each designated treatment, depict a balance between the proportion of ferrite and pearlite achieved after pearlite degeneration.

Appendix 1

To determine average grain diameter (d) of ferrite using the ASTM method, fix a small circular field-of-view of area *a* for counting of grains so that, $a = \pi r^2$ cm^2 $= \dfrac{\pi r^2}{(2.54)^2}$ in^2, *r* being the radius of the field-of-view in centimetre. Now, *n** be the number of times of counting made on the area *a* to cover total area of $n^* a = n^* \dfrac{\pi r^2}{(2.54)^2}$ in^2 and to obtain a total number of grains counted as $\tilde{n}$ (= 500 or more) in a sample at *M* magnification.

Thus, the number of grains per square inch at 100X is $\dfrac{\tilde{n}(2.54)^2}{n^* \pi r^2}\left(\dfrac{M}{100}\right)^2$ so that the average area of one grain at 1X becomes $\dfrac{n^* \pi r^2}{\tilde{n}}\left(\dfrac{1}{M}\right)^2$ cm^2 $= \pi r_0^2$, r_0 being the average radius of the grain at 1X. The above expression yields $r_0 = \sqrt{\dfrac{n^*}{\tilde{n}}} \cdot \dfrac{r}{M}$ cm and $d = 2r_0 = 2\sqrt{\dfrac{n^*}{\tilde{n}}} \cdot \dfrac{r}{M}\ 10^4$ μm.

REFERENCES

[1] ASM Handbook – Properties and Selection: Iron, Steels and High Performance Alloys, Vol.1, (10th Ed.) ASM International, Materials Park, OH 44073-0002, 2008.

[2] M. Thompson, M. Ferry, P.A. Manohar, ISIJ Int. **41**, 891-899 (2001).

[3] X. Fang, Z. Fan, B. Ralph, P. Evans, R. Underhill, Mater. Sci. Technol. **18**, 47-53 (2002).

[4] J.H. Ai, T.C. Zhao, H.J. Gao, Y.H. Hu, X.3. Xie, J. Mater. Proc. Technol. **160**, 390-395 (2005).

[5] P.C.M. Rodrigues, E.V. Pereloma, D.B. Santos, Mater. Sci. Eng. A **283**, 136-143 (2000).

[6] A.B. Cota, R. Barbosa, D.B. Santos, J. Mater. Proc. Technol. **100**, 156-162 (2000).

[7] J. Kang, C. Xie, Mater. Des. **27**, 1169-1173 (2006).

[8] S. Shanmugam, R.D.K. Misra, T. Mannering, D. Panda, G. Jansto, Mat. Sci. Eng. A **437**, 436-445 (2006).

[9] S. Shanmugam, N.K. Ramisetti, R.D.K. Mishra, T. Mannering, D. Panda, S. Jansto, Mater. Sci. Eng. A **460-461**, 335-343 (2007).

[10] Y. Ohmori, R.W.K. Honeycombe, Trans. Iron and Steel Inst. Jpn. **11**, 1160-1165 (1971).

[11] Y. Ivanisenko, W. Lojkowski, R.Z. Valiev, H.J. Fecht, Acta Mater. **51**, 5555-5570 (2003).

[12] R. Song, D. Ponge, D. Raabe, Scr. Mater. **52**, 1075-1080 (2005).

[13] R. Song, D. Ponge, D. Raabe, R. Kaspar, Acta Mater. **53**, 845-858 (2005).

[14] J.R. Yang, C.Y. Huang, C.S. Chiou, ISIJ Int. **35**, 1013-1019 (1995).

[15] E.V. Pereloma, C. Bayley, J.D. Boyd, Mater. Sci. Eng. A **210**, 16-24 (1996).

[16] A.B. Cota, D.B. Santos, Mater. Charact. **44**, 291-299 (2000).

[17] Y.C. Jung, H. Ueno, H. Ohtsubo, K. Nakai, Y. Ohmori, ISIJ Int. **35**, 1001-1005 (1995).

[18] A. Saha, D.K. Mondal, J. Maity, J. Mater. Eng. Perform. **20**, 114-119 (2011).

[19] E.M. Taleff, C.K. Syn, D.R. Lesuer, O.D. Sherby, Metall. Mater. Trans. A **27A**, 111-118 (1996).

[20] A. Saha, D.K. Mondal, K. Biswas, J. Maity, Mater. Sci. Eng. A **5**, 465-475 (2012).

[21] S. Nag, P. Sardar, A. Jain, A. Himanshu, D.K. Mondal, Mater. Sci. Eng. A **597**, 253-263 (2014).

[22] P. Haasen (Ed.), Physical Metallurgy, 1997 Cambridge University Press, UK.

[23] D. Gaude-Fugarolas, H.K.D.H. Bhadeshia, J. Mat. Sci. **38**, 1195-1201 (2003).

[24] G.R. Speich, A. Szirmae, Trans. Metall. Soc. AIME **245**, 1063-1074 (1969).